BNL Experiment E926
Technical Note No.

Measurement of neutral particle production in proton-induced reactions at 24 GeV/c

M.Grigoriev, Yu.Kudenko, O.Mineev

Institute for Nuclear Research RAS
60 October Revolution Pr.7A, 117312 Moscow, Russia

1 Introduction

This note reports the results of the study of the neutral particle production which was undertaken at BNL B2 line in May-June 1997. Uncertainties in the large angle production of the kaons, neutrons and photons by protons have stimulated the dedicated measurement at the proton momentum of 24 GeV/c.

2 Experiment

Fig. 1 shows a sketch of the set-up used in the measurement of the neutral particles: the beam counter arrangement, TOF wall and BaF_2 detector. The dipole Henry Higgins magnet and chambers from the BNL E802 [1] which were used for the measurement of the charged kaon production are not shown. A Cu hadron calorimeter (4 detectors) was placed behind the BaF_2 detector (not shown in Fig. 1).

2.1 BaF_2 detector

An array of 36 modules of the BaF_2 has been used to detect neutrons and photons. The detector was assembled to form a 6x6 array. Each module has 3.5 cm x 3.5 cm cross section and 35 cm in length. Each crystal was directly coupled to a fast phototube. The array was placed at a distance of 7.4 m from the target at the rotating spectrometer platform behind the plastic time-of-flight (TOF) wall, as shown in Fig. 1. The BaF_2 detector covered the area of about 440 cm^2, or approximately 6.4×10^{-5} of the 4π solid angle.

The signal from each individual crystal is split out in a CAMAC leading edge discriminator module. One part is fed to be discriminated over a given threshold while another one is sent to a charge-sensitive Fastbus ADC, where the signals were integrated within 1 μsec gate. The discriminator generates a current proportional to the input multiplicity. These current outputs are daisy chained for all modules, offering a pulse used for the neutral trigger.

2.2 Beam and Target

A 10 cm long and 4×4 mm^2 cross section platinum piece is used as a production target. The beam spot of 3×3 mm^2 was determined by a small plastic counter (finger counter) placed very close to the front of the target.

2.3 Beam counters

The TOF1 and TOF2 counters located upstream of the target area, the finger and steering counters define the geometry of the proton beam. To reject charged particles which hit the BaF_2 detector, and to form a neutral trigger two veto counters were used: a) a large counter (Int) behind the target (about 0.5 m), b) a veto counter (V_{BaF_2}) in front of the BaF_2 array.

The neutral trigger (NT) required a single beam particle to pass through the beam counters with no particles in veto counters plus a signal in BaF_2 detector during the time window of about 200 ns. The neutral trigger was formed as

$$\mathrm{NT} = \mathrm{TOF}_1\times\ \mathrm{TOF}_2 \times \mathrm{Finger} \times \overline{Int} \times \overline{V_{BaF_2}} \times \mathrm{BaF}_2$$

A time-zero signal used in the off-line analysis is obtained from the two photomultipliers of TOF_2 as

$$T_{start} = 1/2(\mathrm{TOF}_{21} + \mathrm{TOF}_{22}).$$

The number of protons on the Pt target was calculated as a triple coincidence: TOF1$\times$TOF2$\times$Finger.

3 Analysis

3.1 Timing

The timing in the BaF_2 detector was taken from a TDC information of the crystal which had a maximum energy deposit. The TDC scale (resolution of 50 ps/channel) allowed us to measure the time interval of about 200 ns that corresponds to neutron energy of less than 10 MeV. The timing shifts between the photon prompt peaks for different crystals were corrected in an off-line analysis. The timing resolution of BaF_2 varies from 200 to 400 psec (σ) and depends on what type of the PMT is used. There is also some contribution to the time resolution from the beam counters. The TOF spectra (summed over all 36 crystals and normalized to the position of the prompt peak of the crystal No.15) accumulated with the neutral trigger at 38.5° and 46.5° are shown in Figs. 2 and 3, respectively. After applying a time-amplitude correction in the off-line analysis we are reached the time resolution of 0.55 ns (σ) for the whole BaF_2 assembly. The prompt peak position corresponds to the photon time-of-flight from the target to the BaF_2 detector. The background subtraction in TOF spectra was obtained by assuming only the constant time-independent background derived from the time region ahead of the prompt photon peak. A contour plot time vs energy at 46.5° is shown in Fig. 4. Neutrons with higher energies (closest to prompt peak) have larger energy deposits in the BaF_2 detector, as seen in Fig. 4.

3.2 Energy calibration

Some part of events induced by the charged trigger in which a charged particle fired the veto counters and TOF wall and then passed through BaF_2 detector was used for the energy calibration of ADC's of BaF_2 crystals. A minimum ionizing particle passing through a 35 cm BaF_2 crystal deposits an energy of about 230 MeV. Unfortunately, the statistics of such events is rather poor that leads to inaccurate calibration of the energy scale. The ADC information was used only for the measurement of the photon energy. Since neutrons deposit only a part of the energy in BaF_2 crystals, the BaF_2 pulse height spectra poorly relate to true neutron energy. The energy spectra observed in the whole detector (after summing around the central crystal over all crystals) are shown in Figs. 5 and 6.

Using time calibration based on the position of the prompt photon signal, the neutron energy was calculated from time-of-flight information. The neutron energy distributions derived from TOF spectra for 38.5° and 46.5° are shown in Figs. 7 and 8, respectively.

3.3 Neutron efficiency of BaF_2 detector

To obtain the neutron flux, the absolute efficiency of BaF_2 detector for detection of fast neutrons is needed. Such an efficiency was measured in Refs. [2, 3]. For $E_n \geq 100$ MeV we used the neutron efficiency $\epsilon_n \sim 0.25$ - 0.3. For neutron energy below 40 MeV the efficiency is less than 0.2 and falls to about zero for neutron energy of $\leq$ 15 MeV [2]. The uncertainty in the BaF_2 efficiency significantly deteriorates the accuracy of the measurement of neutron flux, especially at low energies.

4 Results and discussion

The neutron and photon yields measured at 38.5° and 46.5° are presented in Tables 1, 2 and 3. The neutral flux at 46.5° was measured under different beam intensities which caused a large difference of DAQ dead time. The two results are presented in Table 2 and Table 3. The low intensity proton beam means that the proton intensity on the Pt target was $\sim 1.26\times10^4$ protons/sec. Proton beam intensity was found to be about 1.3×10^5 protons/sec in high intensity run. The number of neutrons and photons detected by BaF_2, normalized neutron and photon yield, the n/p and γ/p ratios, corrected by DAQ dead time, and the n/γ ratio are presented in these tables. The photon thresholds are determined from the calibrated ADC while neutron thresholds are calculated from the TOF spectra. The data obtained at low and high intensity at 46.5° agree reasonably well except for the values with a 10 MeV threshold. The neutron flux was difficult to measure accurately because of the large uncertainty in the neutron detection efficiency of BaF_2.

These results allow us to estimate the photon and neutron flux in E926, where the solid angle of neutral beam is about 2.8×10^{-5} of 4π, i.e. only a factor of two less than the geometrical solid angle covered by the BaF_2 detector. Assuming proton intensity of 5×10^{13} protons/spill, the neutron flux is estimated to be about 5×10^{10} neutrons/spill for neutrons with energies above 10 MeV at both 38.46.5° angles. If the BaF_2 neutron efficiency was underestimated and it can be higher (close to 1), the lower limit of neutron flux is estimated to be at the level of $\sim$(1.5-2.0)$\times10^{10}$ neutrons/spill. For neutron energies greater than 830 MeV (P_n =1.5 GeV/c), the flux decreases by a factor of 20 - 30 at 46.5° and by a factor of 5 - 6 at 38.5°.

For a proposed 20 MHz cavity (2×10^7 microbunches/sec), the estimated number of neutrons (for E_{th} = 10 MeV) is about 1.5×10^3 per microbunch. For neutrons with $P_n \geq$1.5 GeV/c there could be about 50 - 70 neutrons per microbunch at 46.

The photon flux is lower than the neutron one by a factor of 3 - 5. The photon flux from a target can be further reduced by using a Pb filter. However, still there will be about 5-10 photons/microbunch in E926 beam line after using the filter.

5 Conclusion

The results of measurement of neutral particle flux at large angles are presented. The estimated neutron flux with energies above 10 MeV is about 2×10^{-6} n/p$\cdot\mu sr$ and photon flux $\sim 0.4\times10^{-6}$ γ/p$\cdot\mu sr$ at 46.5°.

References

[1] T.Abott et al., A single arm spectrometer detector system for high-energy heavy-ion experiments. NIM, A290 (1990) 41.

[2] R.A.Kryger et al., Efficiency of a BaF_2 scintillator detector for 15-150 MeV neutrons. NIM A346 (1994) 544-547.

[3] V.Wagner et al., Detection of relativistic neutrons by BaF_2 scintillators. NIM A394 (1997) 332-340.

Table 1.

Neutron and photon yield at 38.5°. The total number of protons (p) on a target is 20.6×10^{6}. The dead time of the DAQ is 16 %.

Threshold, MeV	10	50	100	300	830
Number of neutrons, n	8377	7856	6945	4647	2151
Number of photons, γ	16140	8510	6223	3784	1522
n/p	4.07×10^{-4}	3.82×10^{-4}	3.38×10^{-4}	2.26×10^{-4}	1.06×10^{-4}
γ/p	7.83×10^{-4}	4.13×10^{-4}	3.02×10^{-4}	1.84×10^{-4}	0.75×10^{-4}
n/γ	0.52	0.92	1.12	1.23	1.43
After the correction on DAQ dead time					
n/p	4.84×10^{-4}	4.54×10^{-4}	4.02×10^{-4}	2.69×10^{-4}	1.26×10^{-4}
γ/p	9.32×10^{-4}	4.92×10^{-4}	3.59×10^{-4}	2.19×10^{-4}	0.89×10^{-4}
After the correction on neutron efficiency and DAQ dead time					
n/p	2.47×10^{-3}	2.06×10^{-3}	1.78×10^{-3}	1.08×10^{-3}	0.42×10^{-3}
n/γ	2.65	4.17	4.96	4.92	4.72

Table 2.

Neutron and photon yield at 46.5° for the high intensity beam. The total number of protons (p) on a target is 3.1×10^{8}. The dead time of the DAQ is 79 %.

Threshold, MeV	10	50	100	300	830
Number of neutrons, n	29321	21019	16079	7289	1480
Number of photons, γ	23390	14890	11360	5341	1171
n/p	0.94×10^{-4}	0.68×10^{-4}	0.52×10^{-4}	0.23×10^{-4}	0.48×10^{-5}
γ/p	0.75×10^{-4}	0.48×10^{-4}	0.37×10^{-4}	0.17×10^{-4}	0.38×10^{-5}
n/γ	1.25	1.41	1.41	1.36	1.26
After the correction on DAQ dead time					
n/p	4.48×10^{-4}	3.23×10^{-4}	2.47×10^{-4}	1.10×10^{-4}	0.23×10^{-4}
γ/p	3.57×10^{-4}	2.29×10^{-4}	1.76×10^{-4}	0.81×10^{-4}	0.18×10^{-4}
After the correction on neutron efficiency and DAQ dead time					
n/p	2.90×10^{-3}	1.54×10^{-3}	1.13×10^{-3}	4.40×10^{-4}	0.77×10^{-4}
n/γ	8.09	6.64	6.47	5.44	4.19

Table 3.

Neutron and photon yield at 46.5° for the low intensity beam. The total number of protons (p) on a target is 60.5×10^6. The dead time of the DAQ is 16 %.

Threshold, MeV	10	50	100	300	830
Number of neutrons, n	15460	13523	10745	4802	995
Number of photons, γ	16503	10600	8117	3944	876
n/p	2.55×10^{-4}	2.23×10^{-4}	1.77×10^{-4}	0.79×10^{-4}	0.16×10^{-4}
γ/p	2.73×10^{-4}	1.75×10^{-4}	1.34×10^{-4}	0.65×10^{-4}	0.14×10^{-4}
n/γ	0.94	1.27	1.32	1.21	1.13
After the correction on DAQ dead time					
n/p	3.03×10^{-4}	2.65×10^{-4}	2.11×10^{-4}	0.94×10^{-4}	0.19×10^{-4}
γ/p	3.25×10^{-4}	2.08×10^{-4}	1.59×10^{-4}	0.77×10^{-4}	0.16×10^{-4}
After the correction on neutron efficiency and DAQ dead time					
n/p	1.64×10^{-3}	1.24×10^{-3}	9.68×10^{-4}	3.76×10^{-4}	0.63×10^{-4}
n/γ	5.10	5.94	6.05	4.84	3.72

Table 4.

Normalized neutron and photon yield

Angle, deg	Particle	Threshold, MeV	Flux ($p^{-1}\mu sr^{-1}$)
38.5	neutron	10	3.06×10^{-6}
	neutron	100	2.17×10^{-6}
	photon	10	1.15×10^{-6}
46.5	neutron	10	2.02×10^{-6}
	neutron	100	1.26×10^{-6}
	photon	10	0.40×10^{-6}

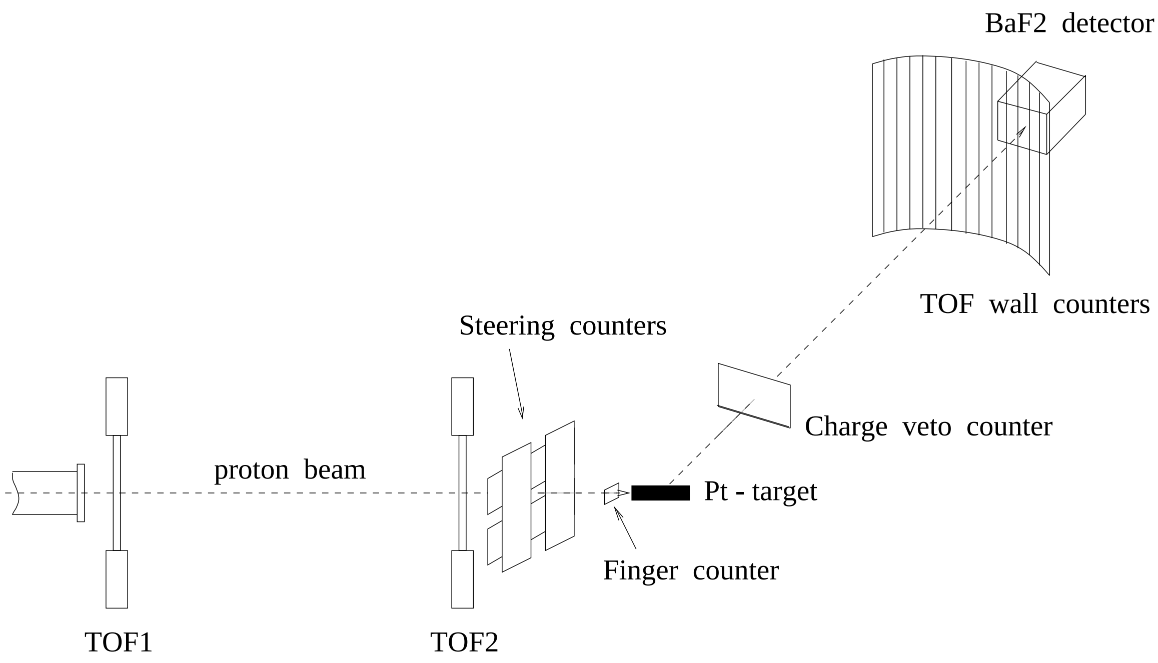

Figure 1: The scheme of the beam counters and BaF_2 array

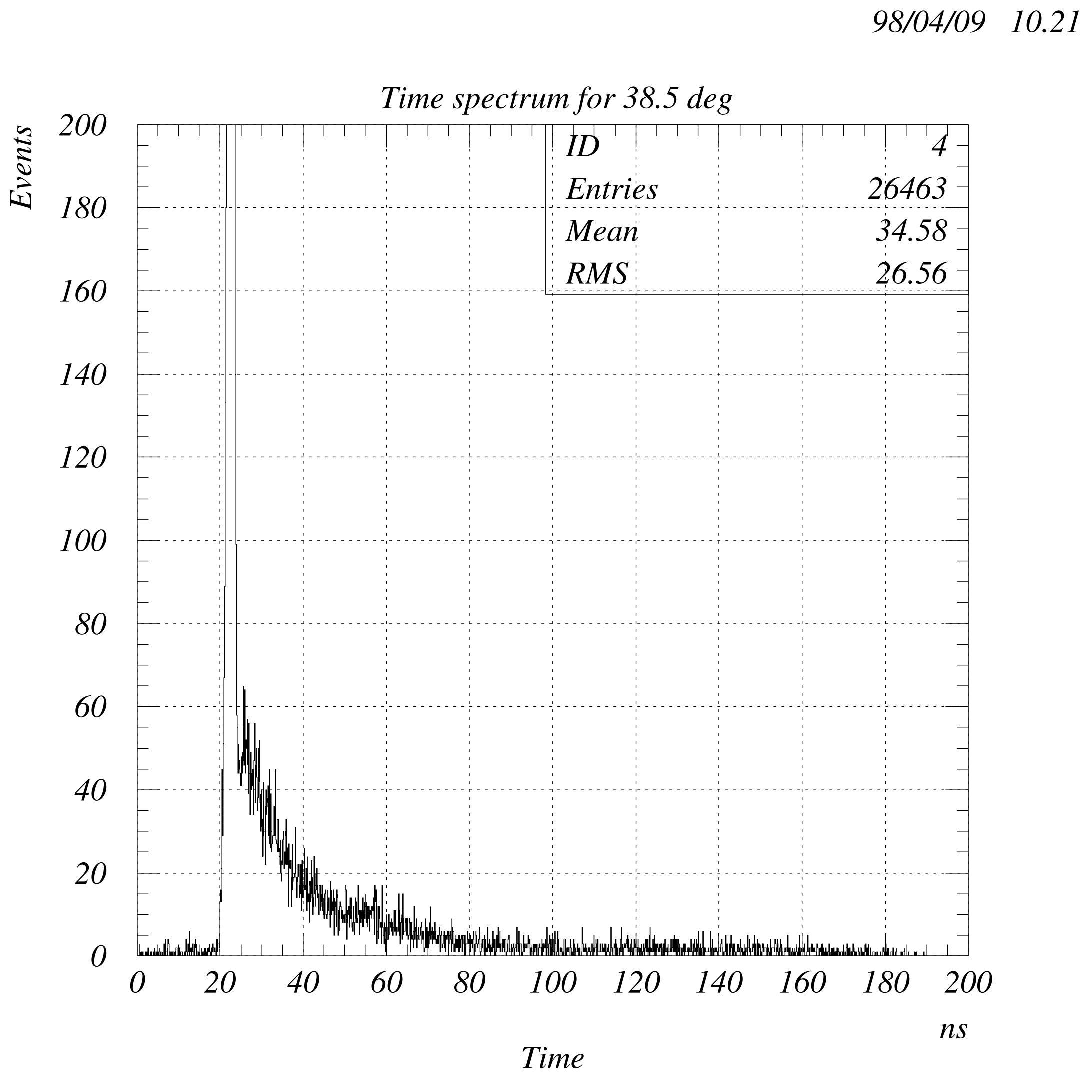

Figure 2: The experimental time-of-flight spectrum (neutral trigger) measured by the BaF_2 array at 38.5°.

.

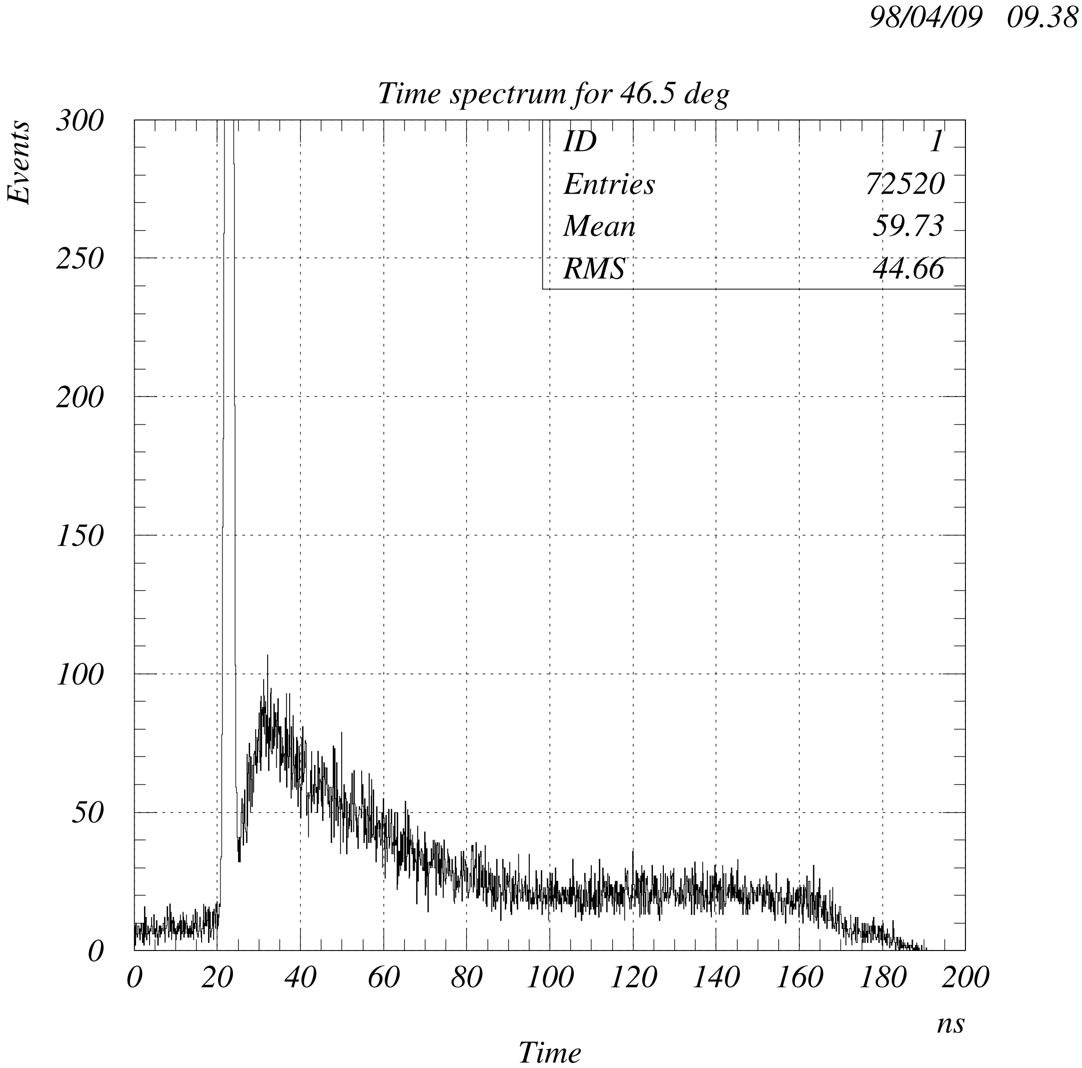

Figure 3: The experimental time-of-flight spectrum (neutral trigger) measured by the BaF_2 array at $46.5°$.

.

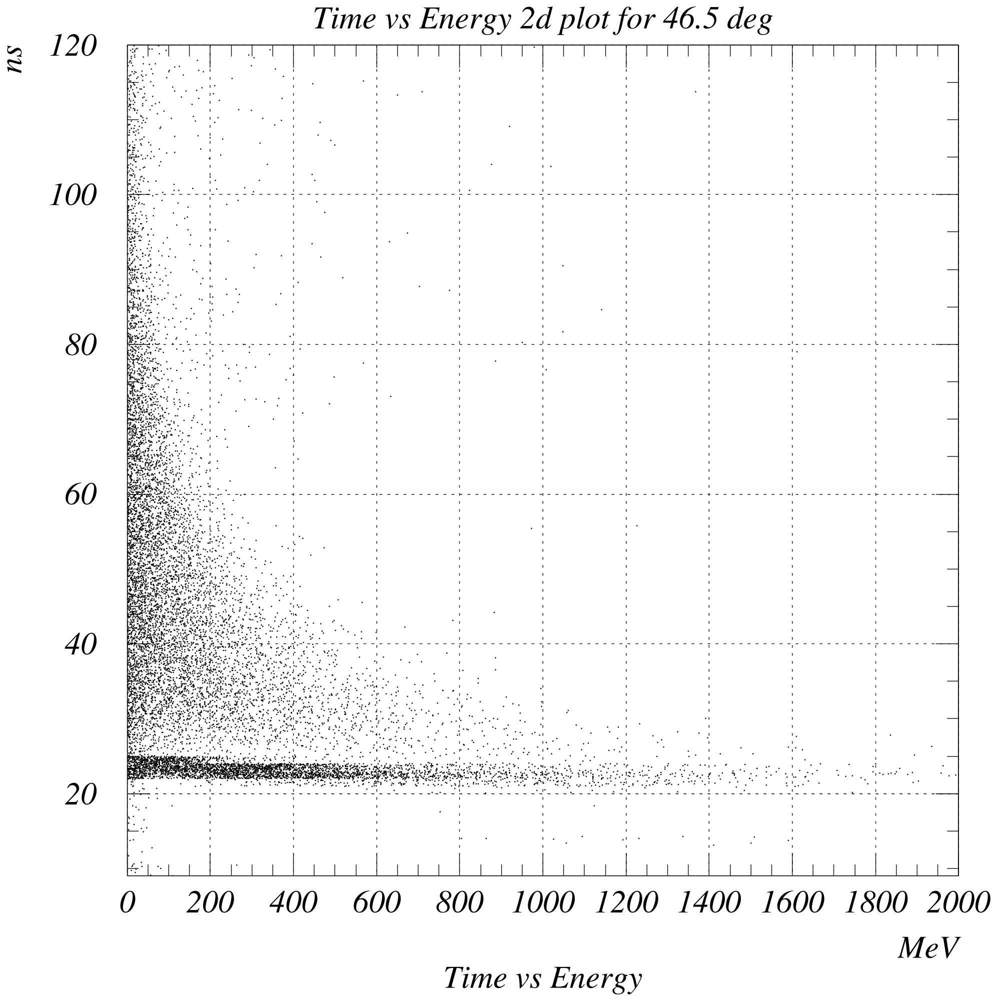

Figure 4: The Time vs Energy 2d plot at 46.5°.

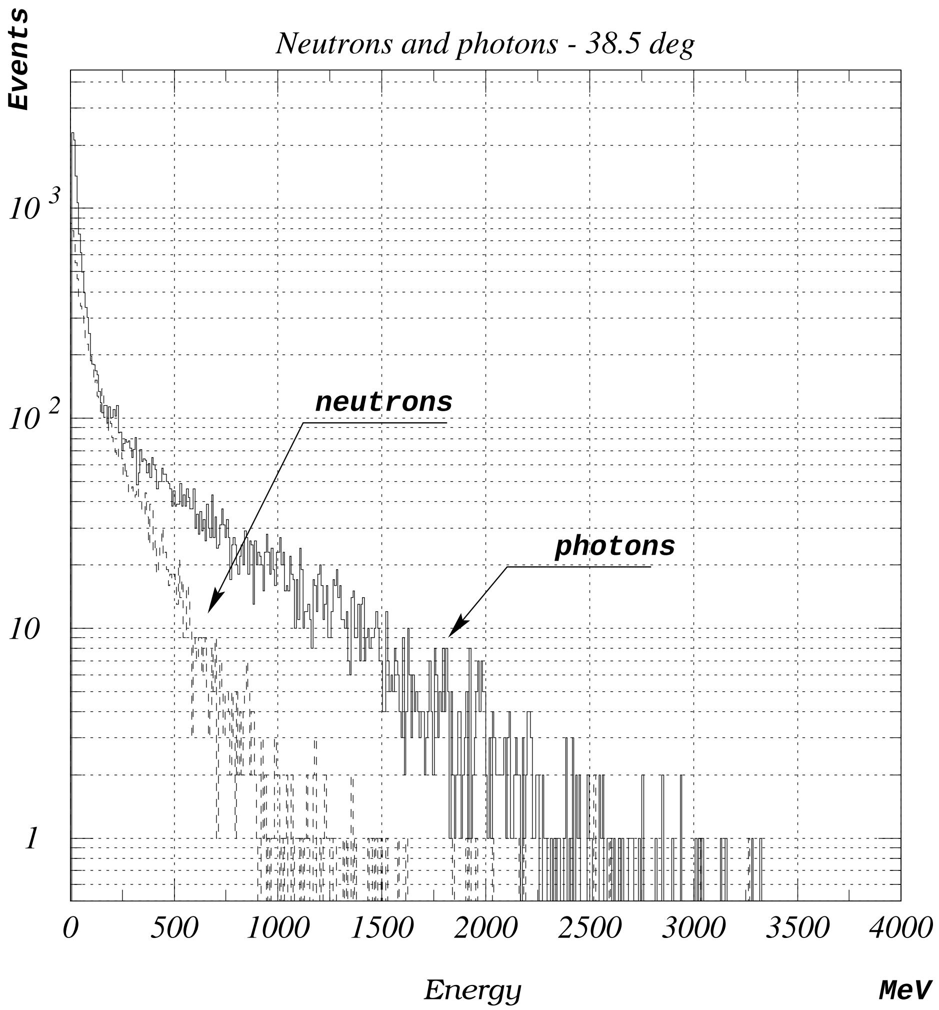

Figure 5: The pulse height spectra of neutrons and photons measured at 38.5°.

.

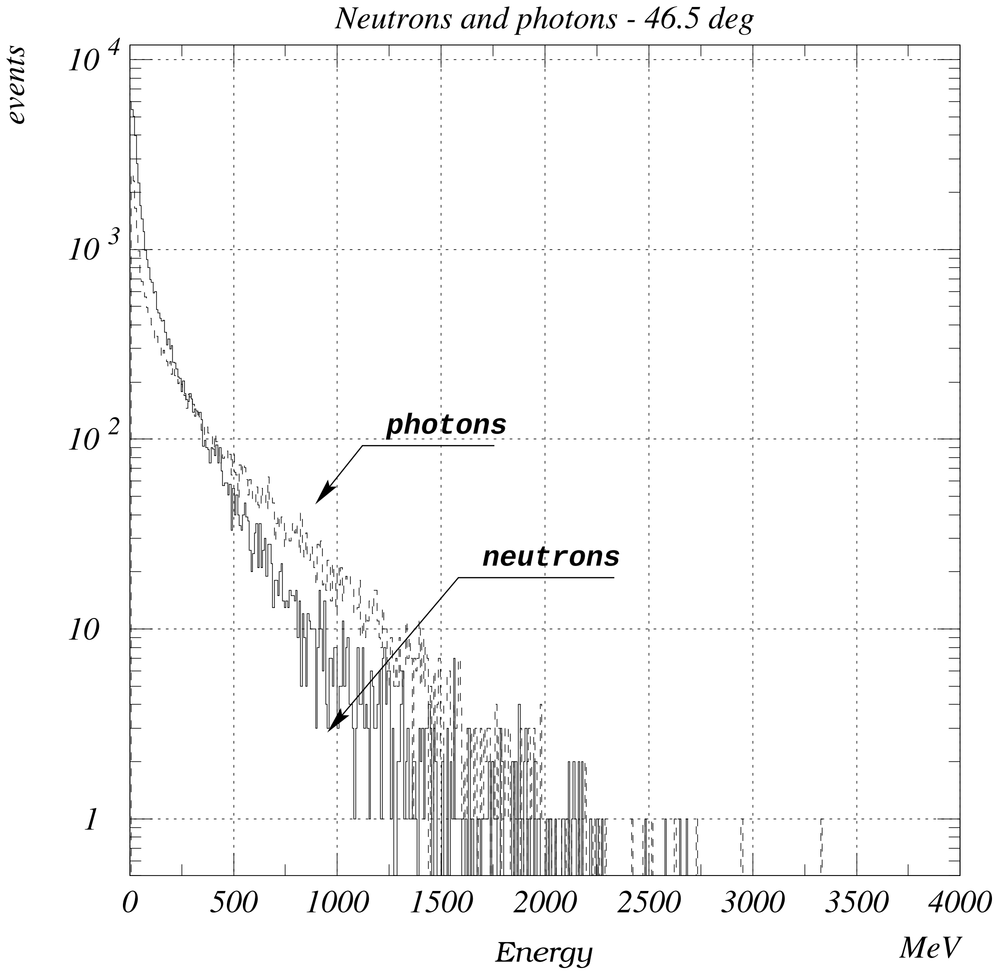

Figure 6: The pulse height spectra of neutrons and photons measured at 46.5°.
.

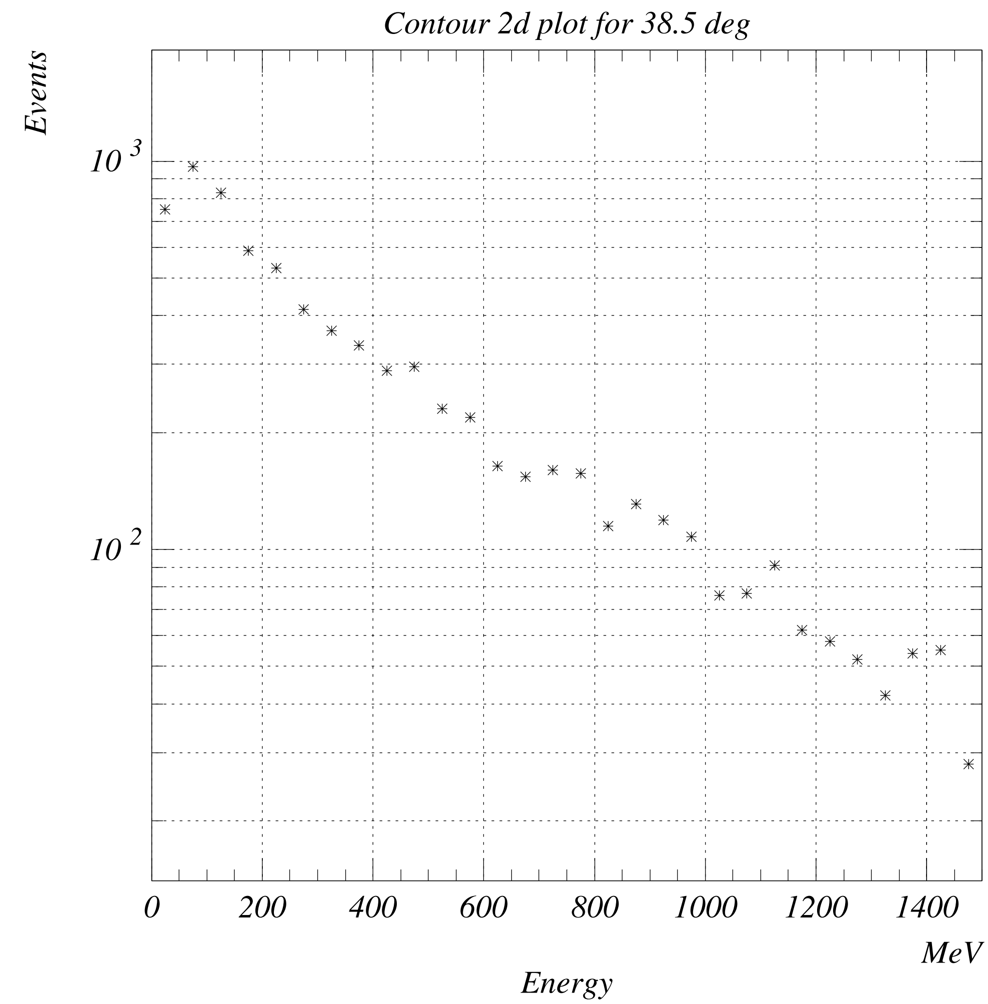

Figure 7: The calculated pulse height spectra at 38.5°. The bin size is 50 MeV.
.

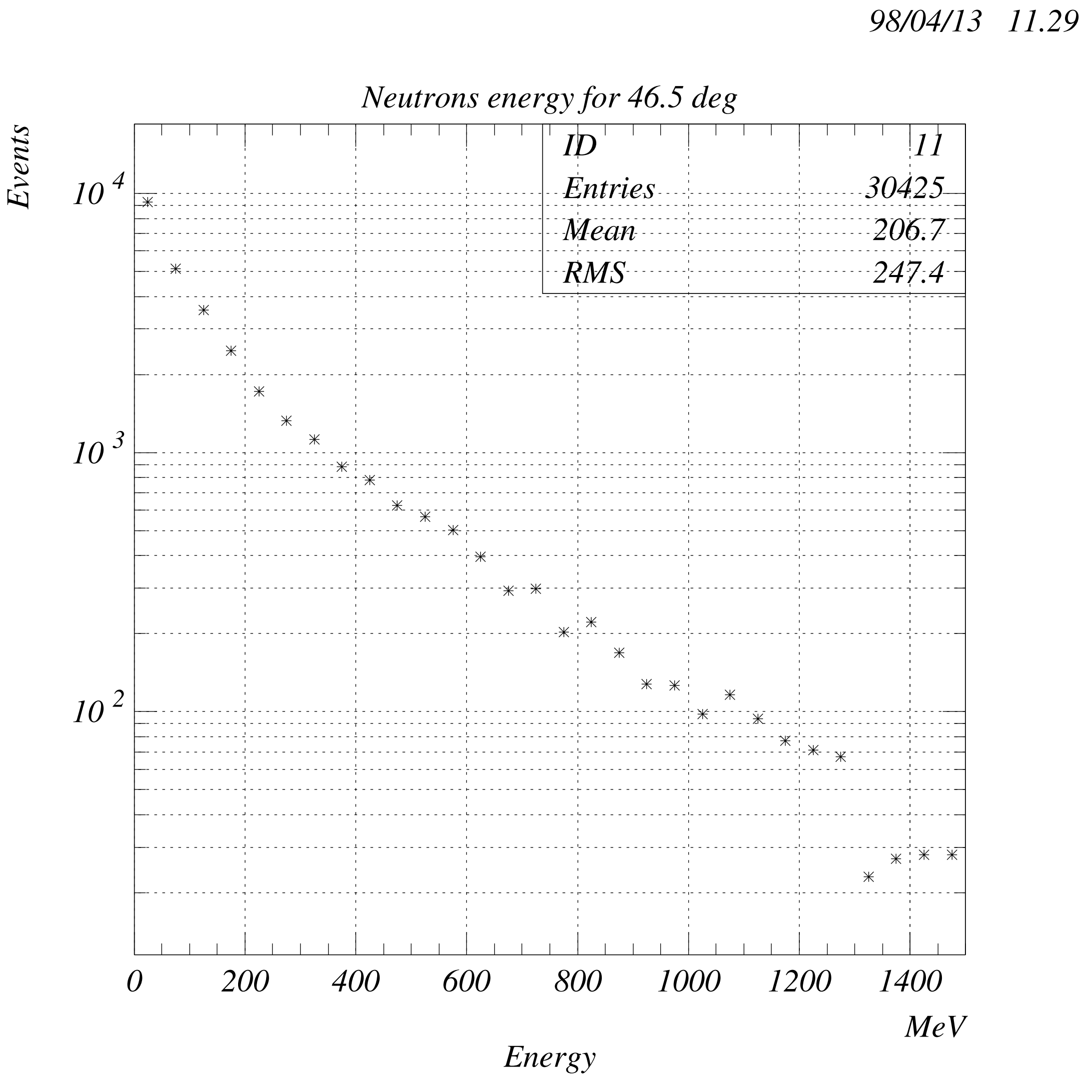

Figure 8: The calculated pulse height spectra at 46.5°. The bin size is 50 MeV
.